



**HAL**  
open science

# Non-Fourier heat transfer at small scales of time and space

Jean-Paul Caltagirone

► **To cite this version:**

Jean-Paul Caltagirone. Non-Fourier heat transfer at small scales of time and space. International Journal of Heat and Mass Transfer, 2020, 160, pp.120145. 10.1016/j.ijheatmasstransfer.2020.120145 . hal-02901385

**HAL Id: hal-02901385**

**<https://hal.science/hal-02901385>**

Submitted on 17 Jul 2020

**HAL** is a multi-disciplinary open access archive for the deposit and dissemination of scientific research documents, whether they are published or not. The documents may come from teaching and research institutions in France or abroad, or from public or private research centers.

L'archive ouverte pluridisciplinaire **HAL**, est destinée au dépôt et à la diffusion de documents scientifiques de niveau recherche, publiés ou non, émanant des établissements d'enseignement et de recherche français ou étrangers, des laboratoires publics ou privés.

# Non-Fourier heat transfer at small scales of time and space

Jean-Paul Caltagirone

Bordeaux INP - University of Bordeaux  
I2M Institute, UMR CNRS n° 5295  
16 Avenue Pey-Berland, 33607 Pessac Cedex  
[calta@ipb.fr](mailto:calta@ipb.fr)

## Abstract

Heat transfer at small spatial and temporal scales presents differences compared to larger scales, where the Fourier law applies with very good representativeness. The best-known deviation concerns the behavior of materials with a very small time constant, where the Fourier law leads to a paradox. But there is another difficulty linked to the writing of the flux as derived from a single scalar potential. Like any vector, the heat flux is the sum of two components, one with curl-free and another with divergence-free, formally as a Hodge-Helmholtz decomposition.

Discrete mechanics derives an equation of motion based on the conservation of the acceleration on a straight line, where the proper acceleration of the material medium is equal to the sum of the accelerations applied to it. This equation is presented as an alternative to the Navier-Stokes equation for fluid motions, but also reflects the conservation of the heat flux. The formulation proposed on this basis makes it possible to calculate the heat flux and to upgrade the scalar and vector potentials explicitly.

## Keywords

Discrete Mechanics; Acceleration Conservation Principle; Hodge-Helmholtz Decomposition; Fourier law, Non-Linear Heat Transfer

---

NOTE: The final publication is available at Elsevier;

J-P Caltagirone, Non-Fourier heat transfer at small scales of time and space, International Journal of Heat and Mass Transfer, doi:10.1016/j.ijheatmasstransfer.2020.120145, 2020.

---

## 1. Introduction

Heat transfer at small scales raises different questions depending on whether they are temporal or spatial scales. The first category relates to the parabolic nature of the heat developed from Fourier's law, leading to the paradox of an infinite propagation celerity. The second problem is the fact that this Fourier law formulated from a thermal potential gradient leads to an irrotational flow. These two problems sometimes meet for industrial applications in micrometric heat transfer.

Heat transfer at very small time scales necessarily leads to an infinite flux when the medium is subjected to a sudden temperature increment. In the middle of the last century, Cattaneo [1], [2] and Vernotte [3], [4] provided a satisfactory response by transforming the heat equation into a hyperbolic version called the Cattaneo-Vernotte model or equation. With the development of micro-thermics and nanomaterials, new Non-Fourier models have emerged; a good number are versions derived from that of Cattaneo and Vernotte, while other ideas based on an analogy with the equations of Maxwell or Navier-Stokes appeared a few decades ago. Let us cite in particular the Thermomass theory developed by several authors including Dong and Guo [5], derived from the theory of special relativity. The review by Khayat [6] gives a good overview of these theories and the physical context to which they apply as a function of the relaxation times of the diffusion effects on small scales. Many works on this topic in relation to nanomaterials have been published in recent years, for instance those of Wang [7].

The use of analogies with Maxwell or Navier-Stokes equations raises the problems of relativity and material indifference. Chistov [8] provides an answer on the latter using a convective derivative, which allows him to derive a scalar equation of heat which satisfies the condition of objectivity. This notion of objective derivative, widely used for complex fluids, is still a subject of controversy, but the principle according to which a constraint, whatever its nature, must be independent during a change of reference system is perfectly legitimate [9]. Maxwell's equation is invariant if we apply a Lorentz transformation where the factor  $\gamma = 1/\sqrt{1 - v^2/c^2}$  induces the principle of causality, the impossibility for a particle or a medium to reach and exceed the celerity of light; the Fourier model contradicts this principle. The Cattaneo-Vernotte model overcomes this difficulty by introducing the essential notion of finite celerity through a relaxation time constant. More recent work [10], [11] is based on a description of heat transfer by the linearized Boltzmann transport equation for the phonon. They show how viscosity and conductivity are set to obtain two coupled equations for the temperature and drift-velocity fields. Their formulation associates momentum and energy to generalize Fourier's heat equation to convective transfers.

The problem of very small scales of space remains even in a stationary regime; the choice to link the heat flux only to the temperature gradient immediately eliminates the effects of transverse heat propagation. The main objective of this contribution is to show that discrete mechanics makes it possible to restore behaviors relating to heat transfer according to the approximations assumed. The approach adopted here is that of discrete mechanics [12], based on the abandonment of the notion of continuum in favor of a discrete vision of space and time. The equation of motion which is derived from it is used to find the results of the Navier-Stokes equation and that of Navier-Lamé by eliminating certain *artefacts*, notably on Stokes law and the non-determination of the viscosity coefficient of compression for fluids [13]. This equation of motion is based on the Hodge-Helmholtz decomposition of the acceleration  $\boldsymbol{\gamma}$  of the material medium or of a particle, and states that this proper acceleration is the sum of the accelerations applied to it, written in the form of two curl-free and divergence-free contributions:

$$\boldsymbol{\gamma} = -\nabla\phi + \nabla \times \boldsymbol{\psi} \quad (1)$$

where  $\phi$  is the scalar potential of acceleration and  $\boldsymbol{\psi}$  is its vector potential. The objective adopted here is to show that this law (1) is also the one which translates the heat flux by diffusion and advection at all spatial and temporal scales.

## 2. Discrete formulation

The discrete mechanics developed in recent years [12] is based on the abandonment of the notion of continuous medium, replacing it by a discrete geometric topology formed of interconnected segments where vectors and scalars are located. The equation derived on this basis translates the conservation of the acceleration considered as an absolute quantity. Numerous examples in fluid and solid mechanics show that this makes it possible to restore the solutions of the Navier-Stokes and Navier-Lamé equations [13].

### 2.1. Acceleration-energy formulation

The geometric topology created in discrete mechanics corresponds to the stencil in figure (1). A straight oriented edge  $\Gamma$  of length  $d$  and of unit vector  $\mathbf{t}$  is limited by two points  $a$  and  $b$ ; three of these segments define the primal topology, a contour  $\Gamma^*$  and a planar facet  $\mathcal{S}$  of oriented unitary normal  $\mathbf{n}$ . The dual planar surface  $\Delta$  joins the barycentres of the cells formed by the set of facets  $\mathcal{S}$  having the edge  $\Gamma$  in common. The unit vectors are thus orthogonal by construction  $\mathbf{t} \cdot \mathbf{n} = 0$ ; a third unit vector  $\mathbf{m}$  orthogonal to the other two makes it possible to construct a local reference frame  $(\mathbf{m}, \mathbf{n}, \mathbf{t})$  for each of the primal facets. Acceleration and velocity, or rather their components, are defined on each edge where they are considered to be constant. The scalar

quantities, like the scalar potential  $\phi$  or the mass, are attached to the vertices  $a$  or  $b$  of the primal geometry, and the same goes for the divergence of the velocity  $\nabla \cdot \mathbf{V}$ . The primal curl  $\nabla \times \mathbf{V}$ , calculated as the circulation of the velocity vector along the contour  $\Gamma^*$ , is carried by the unit normal  $\mathbf{n}$ . The gradient operator  $\nabla\phi$  is simply defined on the segment  $\Gamma$  as a difference of potential at the extremities, and the dual curl  $\nabla \times \boldsymbol{\psi}$  projects the results of the circulation along the contour of the facet  $\Delta$  on the segment  $\Gamma$ .

The tessellation of the physical domain is carried out from this element to form geometric topologies of dimension two or three, based on polygons or polyhedra with any number of facets. Whatever the geometry, the properties  $\nabla_h \cdot \nabla_h \boldsymbol{\psi} = 0$  and  $\nabla_h \times \nabla_h \phi = 0$ , where the index  $h$  designates the discrete operators, are verified exactly, irrespective of the continuous functions  $\phi$  and  $\boldsymbol{\psi}$ . In addition, the decomposition into a divergence-free and a curl-free is orthogonal on the domain [13].

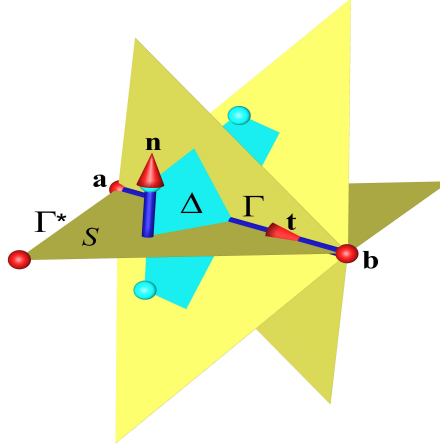


**Figure 1.** Discrete geometric topology from the direct local reference frame  $(\mathbf{m}, \mathbf{n}, \mathbf{t})$ ; a set of primitive planar facets  $S$  are associated with the segment  $\Gamma$  of unit vector  $\mathbf{t}$  whose ends  $a$  and  $b$  are distant by a length  $d$ . Each facet is defined by an contour  $\Gamma^*$  is oriented according to the normal  $\mathbf{n}$  such that  $\mathbf{n} \cdot \mathbf{t} = 0$ ; the dual surface  $\Delta$  connecting the centroids of the cells is also flat.

Deriving the equation of motion is carried out in a single dimension of space on each edge  $\Gamma$ , where a component of the acceleration  $\boldsymbol{\gamma}$  or the other vectors can be considered as scalars assigned to this oriented edge. Contrary to the continuous medium where the notion of conservation requires that of volume, we can attribute to acceleration the property of conservation on this edge. The conservation law of the acceleration  $\boldsymbol{\gamma} = \mathbf{h}$  of the particle or the material medium is written in the form of a Hodge-Helmholtz decomposition:

$$\boldsymbol{\gamma} = -\nabla\phi + \nabla \times \boldsymbol{\psi} \quad (2)$$

where  $\boldsymbol{\gamma}$  is the proper acceleration and where the right-hand side  $\mathbf{h} = -\nabla\phi + \nabla \times \boldsymbol{\psi}$  represents the sum of projections on  $\Gamma$  of the accelerations imposed by the external environment.

The modeling of the phenomena in each of the fields of physics [12] leads to a unique system of equations:

$$\left\{ \begin{array}{l} \boldsymbol{\gamma} = -\nabla (\phi^o - c_t^2 dt \nabla \cdot \mathbf{V}) + \nabla \times (\boldsymbol{\psi}^o - c_t^2 dt \nabla \times \mathbf{V}) + \mathbf{h}_s \\ \alpha_l \phi^o - c_t^2 dt \nabla \cdot \mathbf{V} \mapsto \phi^o \\ \alpha_t \boldsymbol{\psi}^o - c_t^2 dt \nabla \times \mathbf{V} \mapsto \boldsymbol{\psi}^o \\ \mathbf{V}^o + \boldsymbol{\gamma} dt \mapsto \mathbf{V}^o \end{array} \right. \quad (3)$$

where  $c_l$  and  $c_t$  are the longitudinal and transverse celerities of the media concerned, fluid, solid or vacuum; the velocity  $\mathbf{V}$  is a function of the acceleration and the velocity at the previous instant,  $\mathbf{V} = \mathbf{V}^o + \boldsymbol{\gamma} dt$ . The  $\mapsto$  symbol corresponds to an explicit upgrade of the quantity concerned after solving the vector equation of the system (3). The factors  $\alpha_l$  and  $\alpha_t$ , varying between 0 and 1, correspond to the attenuation of the longitudinal and transverse waves, respectively. The source term  $\mathbf{h}_s$ , for example gravitational, capillary effects, etc., will be written in the same way, in the form of a Hodge-Helmholtz decomposition [14]. All the variables and the physical parameters of this system are expressed by the two fundamental units, those of length and time.

The system of equations (3) constitutes a true model with continuous memory. The energies per unit of mass of compression  $\phi^o$  and of shear-rotation  $\psi^o$  are upgraded at each step in time and can be described by the integrals:

$$\phi^o = - \int_0^t c_l^2 \nabla \cdot \mathbf{V} d\tau; \quad \psi^o = - \int_0^t c_t^2 \nabla \times \mathbf{V} d\tau \quad (4)$$

The two main terms of the right-hand side of (3) form two oscillators, each of them a Lagrangian with potential energy stored in  $\phi^o$  (or  $\psi^o$ ) and a velocity-dependent disturbance. These terms, described by a gradient and a dual-curl, are orthogonal and cannot exchange energy directly; the variations of each of them will modify the proper acceleration  $\boldsymbol{\gamma}$  which transfers this acceleration to the other oscillator. In a one-space dimension, for example the longitudinal direction, only the first oscillator will describe the waves of celerity  $c_l$ .

It is also necessary to note the invariance of the right-hand side of the equation (3) with respect to a translation at constant velocity (Galilean transformation), but also for a rotational motion of rigid body; indeed, the operator  $\nabla$  filters these motions and the dual-curl operator of  $\nabla \times \mathbf{V}$  is also reduced to zero. For these two rigid movements the material derivative of the velocity is zero. According to Noether's theorem [15], these invariances reflect the fact that the laws of physics for conducting an experiment remain unchanged and that there is no absolute reference.

The initial instant must correspond to a state of mechanical equilibrium, i.e. the vector equation of the system (3) must be verified identically. In practice it is possible to choose the relative rest state where the movements are associated with a translation or a rotation of rigid body. The proper acceleration is the material derivative  $d\mathbf{V}/dt$  which makes it possible to express the vector equation in terms of velocity and thus to imply all the terms. The nonlinear inertia terms contained in the material derivative will themselves be linearized.

Here the autonomous nature of this formulation should be emphasized; the solution is obtained without any constitutive law or additional conservation law. In particular, conservation of the mass is not necessary to obtain a solution, as is the case for the Navier-Stokes equation to which it is added. This formulation in  $(\boldsymbol{\gamma}, \phi^o, \psi^o)$  makes it possible to evaluate *a posteriori* the velocity, the energy, etc. It presents itself as a law of conservation of energy per unit of mass, where  $\phi^o$  is the compression energy and  $\psi^o$  the shear-rotation energy. The energy-mass duality of the theory of relativity is also found in discrete mechanics, where the conservation of acceleration and energy leads to that of momentum and mass.

The numerical resolution of the system (3) turns out to be particularly robust: (i) the simulations do not depend on any adjustable numerical parameter, (ii) the steady solutions do not depend on the time step chosen, ( $\Delta t = dt$ ), it is only necessary to adjust it so as to capture the physics of the phenomenon, (iii) thanks to the implicitation of all mechanical or thermal effects and constraints applied to the variable  $\mathbf{V}$ , there are no effects due to splitting, as for other numerical techniques. Simple methods of conjugate gradients like BiCGStab2, not preconditioned, make it possible to solve the linear system whose number of unknowns is equal to the number of edges  $\Gamma$ .

## 2.2. Modelling of inertia and advection

The material derivative  $\gamma = d\mathbf{V}/dt$  can make the derivative in time and what will be called inertia  $\kappa_i$  appear in the form  $\gamma = \partial\mathbf{V}/\partial t + \kappa_i$ ; this last term represents the advection of the medium. In a Lagrangian description, by following the particle during its movement the material derivative is equal to the derivative in time. Inertia has a specific form which cannot be deduced from one of those from the continuous medium; it is written:

$$\kappa_i = \nabla \left( \frac{1}{2} \|\mathbf{V}\|^2 \right) - \nabla \times \left( \frac{1}{2} \|\mathbf{V}\|^2 \mathbf{n} \right) \quad (5)$$

The inertia  $\kappa_i$  is presented as the mean curvature of the inertial potential  $\phi_i = \|\mathbf{V}\|^2/2$  defined both on the vertices and on the centroids of the facets of the geometric topology in figure (1); any rotation around  $\mathbf{n}$  of the orthogonal unit vectors  $\mathbf{m}$  and  $\mathbf{t}$  does not modify this mean curvature. The vector  $\kappa_i$  is thus expressed on the edges  $\Gamma$ . In an accelerated motion following a rectilinear trajectory, only the first contribution in gradient of the inertial potential remains and it is not zero.

The superposition of several velocity fields poses no problem for the linear terms of the right-hand side of the equation of motion, but leads to additional non-linear terms for inertia. Let us consider the components  $\mathbf{V}$  and  $\mathbf{W}$  of vectors carried by the segment  $\Gamma$  of unit vector  $\mathbf{t}$ . The norm of this sum is equal to:

$$\|\mathbf{V} \pm \mathbf{W}\|^2 = \|\mathbf{V}\|^2 \pm 2 \|\mathbf{V} \cdot \mathbf{W}\| + \|\mathbf{W}\|^2 \quad (6)$$

Since the vectors  $\mathbf{V}$  and  $\mathbf{W}$  are collinear, we have  $\|\mathbf{V} \cdot \mathbf{W}\| = \|\mathbf{V}\| \|\mathbf{W}\|$  and the vector  $\mathbf{P} = (2 \mathbf{V} \cdot \mathbf{W}) \mathbf{t}$  is also collinear with the other two. By explaining each term as one part curl-free and another part divergence-free, we get:

$$\begin{aligned} \kappa_i = \nabla (\|\mathbf{V} + \mathbf{W}\|^2/2) - \nabla \times (\|\mathbf{V} + \mathbf{W}\|^2/2 \mathbf{n}) &= \nabla (\|\mathbf{V}\|^2/2) - \nabla \times (\|\mathbf{V}\|^2/2 \mathbf{n}) \\ &+ \nabla (\|\mathbf{W}\|^2/2) - \nabla \times (\|\mathbf{W}\|^2/2 \mathbf{n}) \\ &+ \nabla (\mathbf{V} \cdot \mathbf{W}) - \nabla \times (\mathbf{V} \cdot \mathbf{W} \mathbf{n}) \end{aligned}$$

In the general case, the velocity field  $\mathbf{V} + \mathbf{W}$  is obtained from the system of equations (3). If the field  $\mathbf{W}$  is stationary, its divergence null or constant, and its rotational null or constant, the equation becomes:

$$\frac{d\mathbf{V}}{dt} = -\nabla (\phi_R^o - c_t^2 dt \nabla \cdot \mathbf{V}) + \nabla \times (\psi_R^o - c_t^2 dt \nabla \times \mathbf{V}) + \mathbf{h}_s \quad (7)$$

where  $\phi_R^o = \phi^o + \|\mathbf{W}\|^2/2 + \mathbf{V} \cdot \mathbf{W}$  is a new scalar potential and where  $\psi_R^o = \psi^o + \|\mathbf{W}\|^2/2 \mathbf{n} + \mathbf{V} \cdot \mathbf{W} \mathbf{n}$  is a new vector potential. The interest of this notation is to be able to linearize the second member of (7) in velocity  $\mathbf{V}$  to give a form equivalent to (3). Other simplifications are possible depending on the properties of the  $\mathbf{W}$  field. The composition of the inertia term velocities is generic for the interactions of different phenomena in physics. In particular for the heat transfer associated with advection by a fluid,  $\mathbf{V}$  will be the velocity of the fluid and  $\mathbf{W}$  will be the velocity associated with the heat flux.

## 3. Multiscales heat transfer

In continuum mechanics the heat transfer by diffusion and convection is described by the scalar equation of energy associated with the equation of motion, generally the Navier-Stokes

equation. But in discrete mechanics the equation (3) is both an equation of motion and a conservation of energy. The constitutive Fourier law in classical thermodynamics and the conservation law in discrete mechanics are written:

$$\left\{ \begin{array}{l} \boldsymbol{\varphi} = -k \nabla T \\ \frac{d\mathbf{V}}{dt} = -\nabla\phi + \nabla \times \boldsymbol{\psi} \end{array} \right. \quad (8)$$

where  $\boldsymbol{\varphi} = d\phi/dt$  is heat flux density expressed in  $kg s^{-3}$  and  $\phi$  is the energy flux per unit area in  $kg s^{-2}$ . These two laws (8) can be compared formally by assigning specific meanings to the different variables. Table (1) provides the correspondence between the unified variables and the usual thermal variables.

	$\mathbf{V}$	$\phi$	$\boldsymbol{\psi}$	$dt c_l^2$	$dt c_t^2$
Heat Transfer	$(c_p/k) \phi$	$c_p T$	$c_p T \mathbf{n}$	$a_l = k_l/(\rho c_p)$	$a_t = k_t/(\rho c_p)$

**Table 1.** Correspondence between the unified variables and the physical variables of the heat transfer where  $k$  is the thermal conductivity,  $c_p$  the specific heat capacity,  $T$  the temperature,  $a_l$  and  $a_t$  the longitudinal and transverse thermal diffusivities and  $\phi$  the energy flux per unit area.

It should be noted that the usual units of mass (or density) and temperature have disappeared from the units used by the unified variables. All depend only on length and time. In general, the quantities of physics accumulated over time are numerous and sometimes overabundant. Apart from the dimensionless attenuation factors  $\alpha_l$  and  $\alpha_t$ , the only properties to be aware of are the celerities  $c_l$  and  $c_t$ . Table (1) provides them from the measurements already carried out. Thus the system (3) is an equation on the heat flux  $\boldsymbol{\gamma}$  and its potentials  $\phi$  and  $\boldsymbol{\psi}$  but the return to the usual variables is always possible. The processing of the couplings will be ensured by the resolution of several equations, for example natural convection will associate two vector equations, one relating to the field of velocity of the fluid  $\mathbf{V}$  and that representing the heat flux whose velocity is  $\mathbf{W}$ .

### 3.1. Modelling of transverse diffusion

Like Fourier's law, Darcy's, Fick's, Ohm's and Hooke's laws are linear relations built from simple experiments measuring force or flux for a fixed potential difference (temperature, pressure, concentration, electrical potential, deformation, etc.). Rotation effects are therefore excluded from the outset, which inhibits any possibility of finding the corresponding behaviors in the conservation equations into which they are inserted.

Before finding these laws by taking the limit and eliminating the terms of rotation, it is important to show that the transverse heat transfer plays an important role on a small scale of space but also affects the results on a larger scale. Let us consider for this the case of a composite material made up of two solids of length  $L$ , of surface  $S_2$  and of longitudinal thermal conductivity  $k_{l2}$ , arranged on either side of a solid of length  $L$ , of surface  $S_1$  and conductivity  $k_{l1}$ . This stack is subjected to a heat flux generated by a temperature difference  $\Delta T$  maintained on the ends of the three solids. If we name  $\varepsilon_1 = S_1/(S_1 + S_2)$  and  $\varepsilon_2 = 1 - \varepsilon_1$ , then the heat flow in steady state will be equal to  $\Phi = \Phi_1 + \Phi_2 = k^* \Delta T S/L$  where  $k^* = \varepsilon_1 k_{l1} + \varepsilon_2 k_{l2}$  is the equivalent thermal conductivity. Solving the problem from the heat equation would lead to the same result by noting that the temperature whose solution is  $T(x) = \Delta T x$  to a constant; the temperature is thus independent of  $y$ .

The solution obtained from the Fourier law and the heat equation is only an approximation. In fact, the heat fluxes circulating in the two materials are in a ratio  $k_{l1}/k_{l2}$ ; the zones located at

the interfaces between the two media show a discontinuity on the longitudinal fluxes. At small spatial scales this discontinuity generates a non-zero thickness boundary layer and therefore a significant variation in the curl of the heat flux. The Fourier model, limited to only longitudinal fluxes, is unable to account for this phenomenon.

The solution in discrete mechanics is obtained by direct resolution of the equation (3) in two dimensions of space, assuming the periodicity following  $x$  of the heat flux. The fluxes in the two media are generated by a source term  $\mathbf{h}_s = \alpha \mathbf{e}_x$  with  $\alpha = 1$  in the central medium of transverse conductivity  $k_{t1} = 1$  and  $\alpha = 2$  in the conductivity solids  $k_{t2} = 4$ . Figure (2) shows the solutions obtained in the two media corresponding to the problem described above.

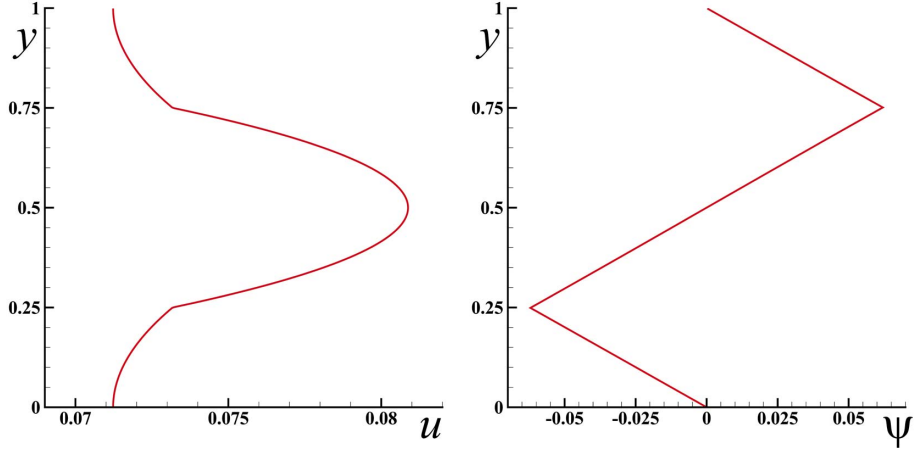


**Figure 2.** Steady heat transfer in a stack of materials with different properties; on the left the evolution of the heat flux  $\mathbf{u}(y)$  following  $y$  and on the right that of the vector potential  $\psi(y)$ .

The velocity field  $\mathbf{W} = u(y) \mathbf{e}_x$  corresponding to the heat flux shows discontinuities on the interfaces located in  $y = 0.25$  and  $y = 0.75$  like that of the vector potential  $dt c_t \nabla \times \mathbf{W}$ . As the solutions correspond to polynomials of degrees less than or equal to two, the result of the numerical solution is exact to machine precision.

To restore the simplified Fourier solution, it is necessary to model this phenomenon by again taking the geometrical topology of figure (1) and replacing the edge  $\Gamma$  by the pipe of figure (3(a)) with radius  $R$ . Let us take for example the case of a cylindrical conducting medium of radius  $R$  subjected to a constant temperature gradient, and assimilate the thermal flux to a Poiseuille flow in a pipe of the same radius. Let us therefore consider the geometry of figure (3 (b)) with  $R = 2r$ , the length of the elementary volume is equal to  $L \gg R$ ; with these definitions, the areas and lengths of the figure are  $\mathcal{S} = DL$ ,  $\Delta = 2\pi r$ ,  $\Gamma_d = 2(D + L)$  and  $\Sigma = \pi r^2$ . The velocity  $\mathbf{W}$  on the pipe will be equal to zero, whereas it is maximum on the axis and twice equal to the velocity for a Poiseuille flow.

The modeling of the rotation term is carried out simply by calculating the primal curl in each of the two cells of a cross section of the plane  $(r, x)$  from the circulation of the velocity vector  $\mathbf{W}$  along the contour  $\Gamma^*$ . This vector is carried by the normal  $\mathbf{n}$  to the plane  $(r, x)$  located at the center of each primal cell. The dual curl is then applied to the vector  $\nu \nabla \times \mathbf{W}$  with  $\nu = dt c_t^2$  using the circulation on the contour  $\Sigma$ . Given the zero velocity of the fluid to the wall, the viscous term becomes:

$$\nabla \times (\nu \nabla \times \mathbf{W}) = \frac{1}{\Sigma} \int_{\Delta} \left( \frac{\nu}{\mathcal{S}} \int_{\Gamma_d} \mathbf{W} \cdot \mathbf{t} dl \right) \cdot \mathbf{n} dl = \frac{2\nu}{r^2} \mathbf{W} \quad (9)$$

where  $\mathbf{W}$  is the velocity on the axis of the pipe  $\Gamma$  or twice the velocity of Darcy  $\mathbf{W}_d$  or the

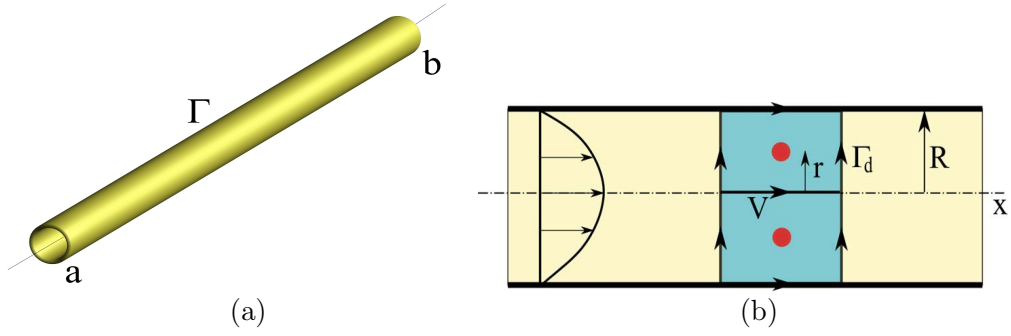


**Figure 3.** Modelization of the diffusion in a thermal conductor by a Poiseuille flow of a fluid of viscosity  $\nu$  on a pipe.

average velocity of flow. Using the diameter of the pipe  $D = 2R$  we find:

$$\nabla \times (\nu \nabla \times \mathbf{W}) = \frac{8\nu}{D^2} \mathbf{W}_d \equiv \frac{\nu}{K} \mathbf{W}_d \quad (10)$$

In the case of a porous medium, through identification, we find that the equivalent permeability is of the form  $K = D^2/8$ . This expression is similar to that of Hele-Shaw in a flat configuration  $K = D^2/12$ . In general, for all phenomena related to diffusion, the modeled term will be written  $-\sigma \mathbf{W}$ , where  $\sigma$  is the equivalent of a resistivity or a resilience whose dimension is in  $s^{-1}$  in SI unit; the quantity  $1/\sigma$  is thus the elapsed time of the phenomenon considered and  $-\sigma \mathbf{W}$  is indeed an acceleration in the opposite direction to that of  $\mathbf{W}$ . In the general case, the resistivity  $\sigma$  becomes a tensor and the scalar product  $\boldsymbol{\sigma} \cdot \mathbf{W}$  is carried, like all the other terms of the equation, by the unit vector of the segment  $\Gamma$ :

$$\begin{cases} \frac{\partial \mathbf{W}}{\partial t} + \nabla \left( \frac{1}{2} \|\mathbf{V} \cdot \mathbf{W}\| \right) - \nabla \times \left( \frac{1}{2} \|\mathbf{V} \cdot \mathbf{W}\| \mathbf{n} \right) = -\nabla (\phi^o - dt c_t^2 \nabla \cdot \mathbf{W}) - \boldsymbol{\sigma} \cdot \mathbf{W} \mathbf{t} \\ \phi = \phi^o - dt c_t^2 \nabla \cdot \mathbf{W} \end{cases} \quad (11)$$

The term of the equation (3)  $\|\mathbf{V} \cdot \mathbf{W}\|$  represents the inertia of the fluid  $\|\mathbf{V}\|^2$  in the case of a flow, but will become  $\|\mathbf{V} \cdot \mathbf{W}\|$  for the advection of  $\mathbf{W}$  by the velocity field  $\mathbf{V}$  in the general case, in particular for the advection of the thermal flux by a flow. The system (11) eliminates the effects of rotation at small spatial scales, which is not yet equivalent to the classic Fourier model because it continues the term of longitudinal propagation which makes the model hyperbolic.

In fact the term  $\nabla \times (\psi^o - dt c_t^2 \nabla \times \mathbf{W})$  always remains valid, with its effects then remaining limited to the areas where the transverse gradients of the heat flux are important. The most realistic equation of motion is to keep the two terms,  $-\nabla \times (dt c_t^2 \nabla \times \mathbf{W})$  and  $-\boldsymbol{\sigma} \cdot \mathbf{W} \mathbf{t}$ .

In this case the solution to the problem with a resistivity equal to  $\sigma = 10^4$  in figure (4) shows the boundary layers of rotation in the neighborhoods of the two interfaces between the media; outside these zones the curl is zero, as in the case of the Fourier model. Even if the effects of shear-rotation in thermal transfer are weak and often negligible in stationary mode, it is probable that situations of strong variations of the thermal flux in unsteady state require a more elaborate physical model than that of Fourier. Generally a vector is always the addition of two components, one solenoidal and the other irrotational; the thermal flux does not escape the application of this theorem. All the phenomena modeled by the gradient of only the scalar potential induce *a priori* a restriction which can become abusive.

The general case of a steady heat transfer on a very small spatial scale thus makes it possible to find the two classic limiting cases (i) that are represented in figure (2), where the transverse

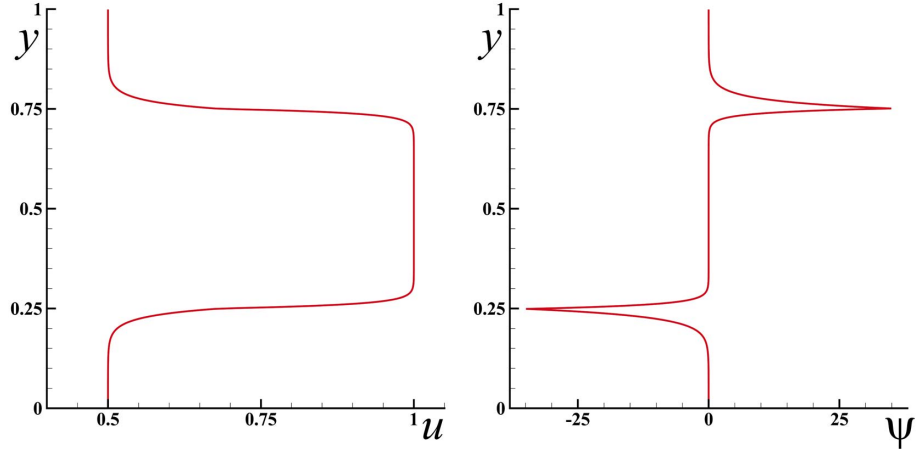


**Figure 4.** Steady heat transfer in a stack of materials with different properties; on the left the evolution of the heat flow  $\mathbf{u}(y)$  following  $y$  and on the right that of the vector potential  $\psi(y)$  multiplied by  $\sigma$ , the value of the resistivity is equal in both medium,  $\sigma = 10^4$ .

propagation effects are dominant and (ii) the one where the classic Fourier solution characterized only by the term in curl-free is present. The solution represented in figure (4) is the general case, even if in practice the thicknesses of thermal boundary layers are difficult to measure.

### 3.2. Heat transfer at small times

This section is devoted to the properties of the discrete equation in one space dimension with weak time constants. Under these same conditions the Fourier law presents a paradox which results in an infinite flux when the medium is subjected to an abrupt variation of temperature. In the absence of the terms of inertia and the term of rotation, the heat equation is written:

$$\begin{cases} \frac{\partial \mathbf{W}}{\partial t} = -\nabla (\phi^o - dt c_l^2 \nabla \cdot \mathbf{W}) - \sigma \mathbf{W} \\ \phi = \phi^o - dt c_l^2 \nabla \cdot \mathbf{W} \end{cases} \quad (12)$$

with  $dt c_l^2 = a_l$  the longitudinal diffusivity,  $\sigma \mathbf{W}$ , the term of transverse diffusion modeled by a longitudinal velocity and  $\phi = c_p T$  the scalar potential. The term  $-\sigma \mathbf{W}$  corresponds to a negative acceleration due to the interactions of phonons in the material. At large time constants, the longitudinal waves are negligible and the Fourier model is thus restored. In short times the behavior of the solution depends on the relative values of  $\sigma$  and  $a_l$ . Figure (5) shows the evolution of the scalar potential (temperature) when an instantaneous unitary variation of it is applied to the edge of the domain in  $x = 0$  when this potential was initially equal to  $\phi = 0$ .

When  $\sigma = 0$ , equation (12) is hyperbolic and the perturbation of the potential propagates without attenuation in the material at a velocity equal to the celerity  $c_l$ , the position of the front is equal to  $x = c_l t$ .

For intermediate values of  $\sigma$ , the disturbance of the potential diminishes rapidly but the amplitude decreases suddenly to zero for the abscissa  $x > c_l t$ . We find the classical behavior in physics (mechanics, electromagnetism, relativity) whereby the velocity of a disturbance cannot exceed the celerity of the medium (shockwave, limitation of the celerity of light) for a rectilinear trajectory.

For intermediate values,  $\sigma = 2$  for example, the solution consists of two laws:

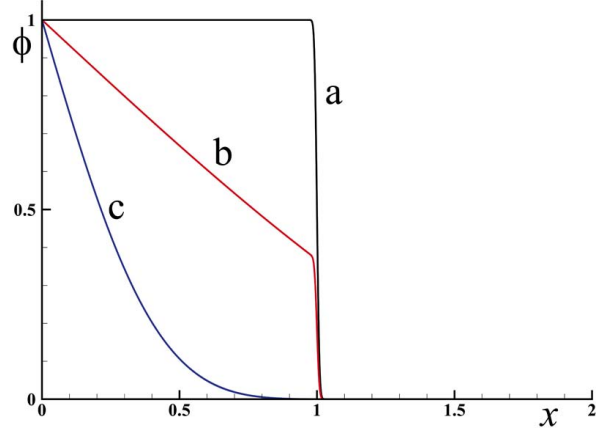


**Figure 5.** Heat transfer by diffusion in a material whose coefficient  $a_l = 1$  for different values of thermal resistivity: (a)  $\sigma = 0$ , (b)  $\sigma = 2$ , (c)  $\sigma = 20$ .

$$\phi(\eta) = \begin{cases} \operatorname{erfc}(\eta) & \text{if } x \leq c_l t \\ 0 & \text{if } x > c_l t \end{cases} \quad (13)$$

For much larger values of  $\sigma$  the longitudinal diffusion is greater and the solution is equal to  $\phi = \operatorname{erfc}(\eta)$  with  $\eta = x/(2\sqrt{a_l t})$ .

In practice, the perturbation propagates well to the celerity  $c_l$  in the material, but the signal is not measurable because the function  $\operatorname{erfc}(\eta)$  decreases very quickly towards zero with  $\eta$ . The accuracy of the solution obtained with the vector system (3) can be evaluated by comparing it to the theoretical solution for  $\sigma = 20$ . In order not to interfere with the convergence in space, the time step chosen is equal to  $dt = 10^{-6} s$  and a Gear scheme of order two is used. The convergence in space is presented in table (2) for a mesh with constant increments varying from  $N = 4$  to  $N = 1024$ . The order of convergence in space in norm  $L_2$  is equal to 2.

$N$	Residue
4	$1.213 \cdot 10^{-2}$
8	$6.390 \cdot 10^{-3}$
16	$1.842 \cdot 10^{-3}$
32	$4.688 \cdot 10^{-4}$
64	$1.203 \cdot 10^{-4}$
128	$3.042 \cdot 10^{-5}$
256	$7.639 \cdot 10^{-6}$
512	$1.911 \cdot 10^{-6}$
1024	$4.762 \cdot 10^{-7}$
Order	2.0

**Table 2.** Heat diffusion: norm  $L_2$  of the residue between the numerical solution resulting from the discrete equation (3) and the theoretical solution  $\operatorname{erfc}(\eta)$ .

The heat flow is limited whatever the time; a simple scaling in order of magnitude of the term  $(\phi^o - dt c_l^2 \nabla \cdot \mathbf{W})$  leads to a calculation of the energy necessary to maintain a potential  $\phi$  in  $x = 0$  [12]. If  $v$  is the norm of  $\mathbf{W}$  we naturally find  $\phi^o = v c_l$  the thermal energy per unit of

mass or  $\phi^o = c_l^2$  if  $v = c_l$  and  $e = m c^2$  if  $e$  is the energy. In fluid mechanics  $\phi^o$  represents the kinetic energy per unit of mass.

#### 4. Natural convection in cavity

The system of equations (3) can be used to calculate the velocity field  $\mathbf{V}$  and the energies of compression  $\phi^o$  and of rotation  $\psi^o$  in a viscous fluid or to calculate the thermal energy density  $\mathbf{W}$ . It can also be used to calculate both the velocity field and the heat flux, taking into account the terms of inertia and the terms of advection of the heat flux by velocity.

This is the case for the problem of natural convection in a differentially heated square cavity, which has been the subject of numerous works [16], [17]. The test case is repeated here for a Rayleigh number equal to  $Ra = 10^5$ . The discrete motion equation is used to obtain the stationary velocity field  $\mathbf{V}$  and the pressure field  $p = \phi^o/\rho$ ; the vector potential is defined by  $\psi^o = \nu \nabla \times \mathbf{V}$  in the case of a Newtonian fluid which does not accumulate viscous stresses ( $\alpha_t = 0$ ). The Archimedes source term translates the gravitational effects applied to a medium of variable densities,  $\mathbf{h}_s = (\rho_v - \rho_m)/\rho_v \mathbf{g}$ . As in the case of convection in open cavities [18], the potential of Bernoulli  $\phi_B^o = \phi^o + 1/2\|\mathbf{V}\|^2$  is used to integrate part of the inertia term in the scalar potential. The thermal flux is represented by the velocity  $\mathbf{W}$  and the thermal energy by  $\phi_h^o = c_p T$ , i.e. the enthalpy. The solution obtained with the discrete model is exactly the same as that which comes from Navier-Stokes and energy equations; the value of the Nusselt number is also equal to the value corresponding to this test case, namely precisely  $Nu = 4.5216$ .

In order to quantitatively validate the physical model and the numerical methodology, a space convergence study was performed on this configuration for structured meshes with a number of cells varying from  $N^2 = 4^2$  to  $N^2 = 1024^2$ . Table (3) shows the evolution of the Nusselt number generally chosen to characterize both the precision of the solution for the dynamic and thermal aspects. Richardson's extrapolation makes it possible to deduce the solution when  $N \rightarrow \infty$  and to calculate the order of convergence, here equal to 2, like the other simulations carried out with this model.

$N$	Nusselt
4	2.122182
8	3.354377
16	4.133262
32	4.413440
64	4.493751
128	4.514615
256	4.519883
512	4.521240
1024	4.521542
$\infty$	4.521643
Order	2.0

**Table 3.** Natural convection in a differentially heated cavity to  $Ra = 10^5$ ; Nusselt number v.s. spatial approximation.

Many other natural convection situations have been studied, particularly in the presence of cavities filled with a fluid and a porous medium [19]. In the latter case, the modeling of the rotation effects presented above can be extended to the thermal and mechanical boundary layers present in the vicinity of the fluid-porous medium interfaces.

The system (3) serves not only to obtain the solution in velocities ( $\mathbf{V}, \mathbf{W}$ ) but also to decompose a vector field into a divergence-free part and another curl-free part. The field  $\mathbf{G} = (\rho_v - \rho_m)/\rho_v \mathbf{g}$  obtained at the end of the previous simulation is used to extract its components  $-\nabla\phi_g$  and  $\nabla \times \psi_g$ . The injection of  $\mathbf{G}$  in the source term of the equation (3) and the resolution of it, with the same boundary conditions as for the initial solution, makes it possible to find the solution on potentials  $\phi_g^o$  and  $\psi_g^o$  to convergence i.e.  $\mathbf{V} = 0$ . These potentials are not those in solving the direct problem,  $\phi^o$  and  $\psi^o$ ; moreover,  $\psi^o = 0$  because a Newtonian fluid does not accumulate shear stresses.

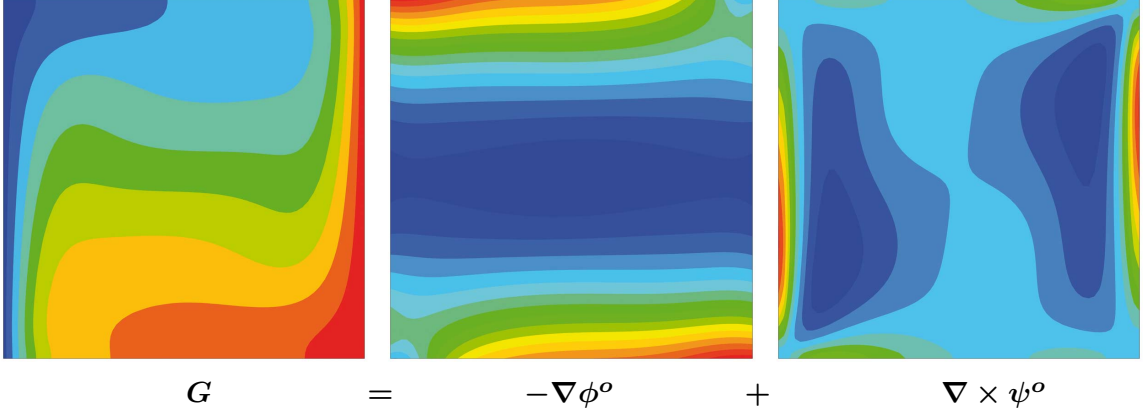


**Figure 6.** Natural convection in differentially heated square cavity at  $Ra = 10^5$ , the source term  $\mathbf{G} = (\rho_v - \rho_m)/\rho_v \mathbf{g}$  is decomposed in curl-free component of scalar potential  $\phi_g$  and divergence-free component of vector potential  $\psi_g$ ; the velocity is  $\|\mathbf{V}\| < 10^{-18}$  at convergence.

Figure (6) shows the density field  $\mathbf{G} \cdot \mathbf{e}_y$  and the scalar and vector potentials of the Hodge-Helmholtz decomposition, which is formally written:

$$\mathbf{G} = \frac{(\rho_v - \rho_m)}{\rho_v} \mathbf{g} = -\nabla\phi_g^o + \nabla \times \psi_g^o \quad (14)$$

Thus the system of equations of discrete mechanics (3) makes it possible to replace the Navier-Stokes and energy equations, but also to extract the scalar and vector potentials of a vector for specified boundary conditions.

## 5. Conclusions

The direct transposition of the equation of motion of discrete mechanics in terms of acceleration and potentials  $(\gamma, \phi, \psi)$  to heat transfer leads to the addition of a Fourier-law non-curl-free term which generalizes it. In fact, like any vector, the heat flow decomposes into an irrotational component and another solenoidal component. While the latter is generally zero at large scales, this is no longer the case at small spatial scales. The resolution of complex industrial problems absolutely does not make it possible to decide *a priori* on the physical model and the equation to be adopted. The discrete equations naturally degenerate towards the right model without advance prejudice to the choice of this model.

From the numerical point of view, the system of equations (3) has remarkable properties of robustness, precision and efficiency without any adjustable parameter. The only physical parameters are the longitudinal and transverse velocities; the elapsed time  $dt$  is chosen according to the physics apprehended, from  $dt \approx 10^{15}$  s for stationary problems to  $dt \approx 10^{-20}$  s for simulate light waves.

From the physical point of view, the abandonment of the mass and momentum of the continuum mechanics does not call into question the conservation of these quantities, as the equation of movement conserves energy and acceleration. By abandoning temperature as a potential, the unit with which it is expressed in all of the unified parameters is eliminated. Length and time are the only fundamental quantities of the unified system of equations.

## References

- [1] C. Cattaneo, Sulla conduzione del calore, *Atti Sem. Mat. Fis. Univ Modena* 3 (1948) 83–101.
- [2] C. Cattaneo, Sur une forme de l'équation de la chaleur éliminant le paradoxe d'une propagation instantannée, *Comptes Rendus Acad. Sciences* 247 (4) (1958) 431–433.
- [3] P. Vernotte, Les paradoxes de la théorie continue de l'équation de la chaleur, *Comptes Rendus Acad. Sciences* 246 (1958) 3154–3155.
- [4] P. Vernotte, Some possible complication in the phenomena of thermal conduction, *Comptes Rendus Acad. Sciences* 252 (1961) 2190–2215.
- [5] Y. Duong, Z. Guo, Entropy analyses for hyperbolic heat conduction based on the thermomass model, *Int. J. Heat Mass Transfer* 54 (2011) 1924–1929. doi:dx.doi.org/10.1016/j.ijheatmasstransfer.2011.01.011.
- [6] R. Khayat, J. de Bruyn, D. Stranges, R. Khorasany, Non-Fourier effects in macro- and micro-scale non isothermal flow of liquids and gases. Review., *Int. J. of Thermal Scien.* 97 (2015) 163–177.
- [7] M. Wang, N. Yang, Z. Guo, Non-Fourier heat conductions in nanomaterials, *Phys. Appl. Physics* 110 (2011).
- [8] C. Christov, On frame indifferent formulation of the maxwell-cattaneo model of finite-speed heat conduction, *Mech. Res. Commun.* 36 (4) (2009) 481–486.
- [9] C. Truesdell, *A First Course in Rational Continuum Mechanics*, Academic Press, New York, 1977.
- [10] A. Cepellotti, N. Marzari, Thermal transport in crystals as a kinetic theory of relaxons, arXiv:1603.02608v3 [cond-mat.mtrl-sci] (2016) 1–16.
- [11] M. Simoncelli, N. Marzari, A. Cepellotti, Generalization of fourier's law into viscous heat equations, *Physical Review X* 10 (2020) 1–35. doi:10.1103/PhysRevX.10.011019.
- [12] J.-P. Caltagirone, *Discrete Mechanics, concepts and applications*, ISTE, John Wiley & Sons, London, 2019. doi:10.1002/9781119482826.
- [13] J.-P. Caltagirone, S. Vincent, On primitive formulation in fluid mechanics and fluid-structure interaction with constant piecewise properties in velocity-potentials of acceleration, *Acta Mechanica* 231 (6) (2020) 2155–2171. doi:10.1007/s00707-020-02630-w.
- [14] H. Bhatia, G. Norgard, V. Pascucci, P. Bremer, The Helmholtz-Hodge Decomposition - A Survey, *IEEE Transactions on Visualization and Computer Graphics* 19 (8) (2013) 1386–1404. doi:10.1109/TVCG.2012.316.
- [15] Y. Kosmann-Schwarzbach, *Nother Theorems. Invariance and Conservations Laws in the Twentieth Century*, Springer-Verlag, New York, 2011. doi:10.1007/978-0-387-87868-3.

- [16] G. de Vahl Davis, Natural convection of air in a square cavity: a bench mark numerical solution, *Int. J. Numer. Meth.* 3 (1983) 249.
- [17] P. Le Quéré, Accurate Solutions to the Square Thermally Driven Cavity at High Rayleigh Number, *Comp. Fluids* 20 (1991) 29–24. doi:[https://doi.org/10.1016/0045-7930\(91\)90025-D](https://doi.org/10.1016/0045-7930(91)90025-D).
- [18] G. Desrayaud, E. Chénier, A. Joulin, A. Bastide, B. Brangeon, J.-P. Caltagirone, Y. Cherif, R. Eymard, C. Garnier, S. Giroux-Julien, Y. Harnane, P. Joubert, N. Laaroussi, S. Lassueb, P. Le Quéré, R. Li, D. Saury, A. Sergent, S. Xin, A. Zoubir, Benchmark solutions for natural convection flows in vertical channels submitted to different open boundary conditions, *International Journal of Thermal Sciences* 72 (2013) 18–33. doi:[10.1016/j.ijthermalsci.2013.05.003](https://doi.org/10.1016/j.ijthermalsci.2013.05.003).
- [19] T. Basak, S. Roy, T. Paul, I. Pop, Natural Convection in a Square Cavity Filled with a Porous Medium: Effects of Various Thermal Boundary Conditions, *International Journal of Heat and Mass Transfer* 49 (2006) 1430–1441. doi:<https://doi.org/10.1016/j.ijheatmasstransfer.2005.09.018>.